Transduction Efficiency of Adeno-Associated Virus Serotypes After Local Injection in Mouse and Human Skeletal Muscle

Laura Muraine, Mona Bensalah, Jamila Dhiab, Gonzalo Cordova, Ludovic Arandel, Alix Marhic, Maud Chapart, Stéphane Vasseur, Sofia Benkhelifa-Ziyyat, Anne Bigot, et al.

Title Page

Transduction efficiency of AAV serotypes after local injection in mouse and human skeletal muscle

Laura Muraine[1], Mona Bensalah[1], Jamila Dhiab[1], Gonzalo Cordova[1], Ludovic Arandel[1], Alix Marhic[1], Maud Chapart[2], Stéphane Vasseur[2], Sofia Benkhelifa-Ziyyat[1], Anne Bigot[1], Gillian Butler-Browne[1], Vincent Mouly[1], Elisa Negroni[1], Capucine Trollet[1]

[1] Sorbonne Université, Inserm, Institut de Myologie, U974, Centre de Recherche en Myologie, 47 Boulevard de l'hôpital, 75013 Paris, France
[2] MyoBank AFM – Institut de Myologie, 47 Boulevard de l'hôpital, 75013 Paris, France

Corresponding author: Capucine Trollet

Corresponding author's address: U974 Inserm – Centre de Recherche en Myologie GH Pitié Salpétrière Bat Babinski 47 bd de l'Hopital 75013 Paris

Corresponding author's phone and fax: 01 42 16 57 15 / 01 42 16 57 00

Corresponding author's e-mail address: capucine.trollet@upmc.fr

Running head: AAV efficiency in mouse and human muscle

Abstract (296 words)

Adeno-associated viral vector (AAV) is an efficient tool for gene delivery in skeletal muscle. AAV-based therapies show promising results for the treatment of various genetic disorders, including muscular dystrophies. These dystrophies represent an heterogeneous group of diseases affecting muscles and typically characterized by progressive skeletal muscle wasting and weakness and the development of fibrosis. The tropism of each AAV serotype has been extensively studied using systemic delivery routes, but very few studies have compared their transduction efficiency via direct intramuscular injection. Yet, in some muscular dystrophies, where only a few muscles are primarily affected, a local intramuscular injection to target these muscles would be the most appropriate route. A comprehensive comparison between different rAAV serotypes is therefore needed. Here, we investigated the transduction efficiency of rAAV serotypes 1 to 10 by local injection in skeletal muscle of control C57BL/6 mice. We used a CMV-nls-LacZ reporter cassette allowing nuclear expression of LacZ to easily localize targeted cells. Detection of beta-galactosidase activity on muscle cryo-sections demonstrated that rAAV1, 7, 8, 9 and 10 were more efficient than the others with rAAV9 being the most efficient in mouse. Furthermore, using a model of human muscle xenograft in immunodeficient mice, we observed that in human muscle rAAV8 and rAAV9 had similar transduction efficiency. These findings demonstrate for the first time that human muscle xenograft can be used to evaluate AAV-based therapeutical approaches in a human context.

Introduction

Adeno-associated virus (AAV) recombinant vectors (rAAV) are tools of choice for a wide range of gene therapy applications in humans, due to their good safety profile in clinical trials including an ability to transduce both dividing and non-dividing cells, to elicit a limited cytotoxicity [1] and to allow long-term transgene expression.[2]. Many serotypes of AAV from human and primate source have been identified, including AAV1 [3], AAV2 [4], AAV3 [5], AAV4 [6], AAV5 [7], AAV6 [8], AAV7 [9], AAV8 [9], AAV9 [10], AAV10 [11], each of them with a specific transduction and tropism profile. Recombinant AAV (rAAV) have been shown to efficiently infect many tissues including liver [12,13]; lung [14], eye [15] and skeletal muscle [16,17], their tissue transduction targeting being dependent both on the capsid properties[18] and the route of administration [2].

Skeletal muscles constitute 40-50% of the body mass in adult humans, and encompasses a broad range of different muscles. Each of these muscles is composed of contractile muscle fibres, post-mitotic multinucleated cells, surrounded by a specialized plasma membrane - the sarcolemma - and by a layer of extracellular matrix known as the basement membrane. Tropism evaluation of rAAV serotypes in muscle has mainly been studied by systemic administration: rAAV1, 6, 7, 8 and 9 showed efficient transduction of skeletal muscle in most animal models[19–21]. But to our knowledge, no study has provided a comprehensive side-by-side comparison of the transduction efficiency and pattern of serotypes 1 to 10 after a direct *in vivo* local intramuscular injection, a route of delivery needed in some cases of muscular dystrophies where discrete muscles need to be targeted.

Muscular dystrophies are a heterogeneous group of genetic disorders characterized by progressive muscle wasting and weakness. These diseases are often associated with an excessive accumulation of extracellular matrix leading to muscle fibrosis. This is for example the case in Duchenne muscular dystrophy (DMD), where mutations in the dystrophin gene lead to cycles of degeneration/regeneration and the eventual development of fatty infiltration and fibrosis. This is also the case for a much rarer disease called oculopharyngeal muscular dystrophy (OPMD) where an abnormal triplet expansion in the *PABPN1* gene [22] leads primarily to pharyngeal and eyelid muscle weakness and exacerbated fibrosis in these affected muscles [23]. Regarding OPMD, promising preclinical AAV-based gene replacement therapy data have been obtained via intramuscular injection in an OPMD mouse model [24] and the AAV gene-replacement product has now received orphan drug designation from EAM and FDA. Whereas a whole-body transduction efficiency has to be reached for DMD - three AAV

trials for DMD are on going in the US based on the delivery of various engineered micro-dystrophins via systemic delivery using rAAV9 and rAAVrh74 [25] (NCT03368742 Solid Biosciences; NCT03375164 Nationwide Children's Hospital; NCT03362502 Pfizer) [2] in OPMD patients, a local intramuscular injection would probably be preferred since a restricted number of muscles are primarily affected.

Fibrotic muscular substitution is a complex process characterized by an excessive accumulation of collagens and other components of ECM [26] surrounding muscle fibers and fibroblasts that have an increasingly appreciated role as an autocrine source of profibrotic stimuli [27]. The capacity to target fibrotic interstitial cells with rAAV has never been evaluated. In this study, we evaluated the transduction efficiency of rAAV serotypes following intramuscular injection. Furthermore, we investigated the transduction translatability into human skeletal muscle, using a model of human muscle xenograft into immunodeficient mice allowing a side-by-side comparison in mouse and human context, an essential step for preclinical therapeutic studies.

Material and Methods

AAV production

AAV pseudotyped vectors containing a CMV-nlsLacZ expression cassette were produced using a three plasmid transfection in HEK-293 cells as described previously [28] using the pAAV-CMV-LacZ plasmids with the pXX6 plasmid coding for the Ad helper genes essential for AAV production and the pRepCap plasmid coding for AAV capsids. Vector particles were purified on an iodixanol gradient and concentrated on Amicon Ultra-15 100 K columns (Merck-Millipore). The titer corresponding to the number of viral genomes per milliliter (vg/ml) was determined by quantitative real-time PCR on a StepOnePlus (Applied Biosystems), by using the following primers and probe: CTCCATCACTAGGGGTTCCTTG (forward), GTAGATAAGTAGCATGGC (reverse) and TAGTTAATGATTAACCC (Taqman MGB probe, Life Technologies) amplifying a region between the ITR and the promoter. The pAAV plasmid was used as a control to establish the standard curve for absolute quantification.

In vivo injection

3 month old male C57BL/6J (Janvier Labs) mice were injected in the tibialis interior (TA) with the different AAV serotypes (containing 3.5×10^{10} vg per injection) diluted in 25μl PBS using a Hamilton syringe. Injections were carried out under general anesthesia using xylasine (80 mg/kg) /ketamine (10 mg/kg). Animal studies conform to the French laws and regulations concerning the use of animals for research and were approved by an external Ethical committee (approval no.16650-2018090514008520 delivered by the French Ministry of Higher Education and Scientific Research).

Muscle analysis

Four weeks post-injection mice were sacrificed by cervical dislocation; TA muscles were collected and snap-frozen in liquid nitrogen-cooled isopentane. Transverse 5μm sections were made with a cryostat (Leica CM1850) throughout the whole muscle with 500 μm between each section (**supp figure 1A**). Additional tissue between the sections was collected for DNA and/or protein extraction, ensuring representation of the whole muscle during data collection.

Xenografts

Three to four month old male or female immunodeficient Rag2−/− Il2rb−/− mice were used as recipients for human xenografts. Control donor human tensor Fascia Lata muscle was cut

into strips (8x3x1mm). Mice were anaesthetized with an intraperitoneal injection of ketamine hydrochloride (80 mg/kg) and xylazine (10 mg/kg) (Sigma-Aldrich, St Louis, MO) in accordance with the French and European Community legislation (approval no. 4165-2016021715164682 delivered by the French Ministry of Higher Education and Scientific Research). The TA and extensor digitorum longus (EDL) were removed. Human muscle samples were obtained as surgical waste during routine surgical procedures from the MYOBANK, a tissue bank affiliated to EuroBiobank (authorization from the French Ministry ref 2013-1968) after all subjects had signed informed consent. The strip of human muscle was placed in the empty anterior compartment and tied, at both ends, with non-absorbable suture (Ethicon) to the tendons of the peroneus longus. Skin was sutured with absorbable suture (Ethicon). Buprenorphine (0.1 mg/kg) was given subcutaneously at the beginning of the surgery and each 12 hours (h) for the first 48h after surgery, for pain control. 4 months after surgery, when the human muscle was fully regenerated, the grafts were injected with the different AAV serotypes as described previously.

β-galactosidase histochemistry and histological analysis

Muscle sections were fixed with 0,25% glutaraldehyde for 5 minutes and stained for several hours with a mixture of 500 µg/mL X-Gal (5-bromo-4-chloro-3-indolyl-β-D-galactopyranoside), 5 mM potassium hexacyanoferrate(III), 5mM potassium hexacyanoferrate(II) trihydrate, and 2 mM magnesium chloride in PBS at 37°C. Laminin staining was performed by incubating the sections in H2O2 3% for 5 min, then blocking in FBS 2% for 30 min and incubating with anti-laminin antibody (1:400 diluted in PBS, Z0097, Dako, Agilent Technologies France, Les Ulis, France) and the biotinylated secondary antibody (1:200 diluted in PBS, E0432, Dako). Laminin staining was revealed with Diaminobenzidine with 0,01% H_2O_2. For the assessment of tissue morphology and visualization of fibrosis and connective tissue, muscle sections were stained with hematoxylin and eosin and sirius red for light microscopic examination. Pictures were taken with a slide scanner (Hamamatsu). For each muscle, we selected the largest cross section area among all the muscles sections of a TA muscle and on this section we counted the total number of β-gal–positive nuclei. The relative transduction efficiency was calculated as βgal positive nuclei/mm2/gc, with the genome copy (gc) number calculated as per µg DNA (see below).

Western-blot analysis

Proteins were extracted from muscle sections by sonicating the cells in RIPA buffer (0.15 M NaCl, 0.1% SDS, 50 mM Tris-HCl (pH 8), 2 mM EDTA and 10% Triton-X-100 with protease inhibitor cocktail (Complete, Roche Diagnostics) and phosphatase inhibitor cocktail (Santa Cruz; sc-45064). Protein concentration was determined by colorimetric detection method (Pierce BCA Protein Assay; Thermo Fisher). Proteins were separated on 4–12% Bis–Tris gels (Invitrogen) and transferred onto a PVDF membrane for 1 h at constant 250 mA at 4°C. Membranes were blocked by incubation in 5% BSA in 1X TBS, 0.1% Tween-20 (TBST) for 1h at room temperature under agitation. Membranes were stained with anti-beta galactosidase antibody (Thermofisher A-11132 ; 1 :1000 1 hour) and tubulin antibody (Sigma T5168 1 :1000 1 hour). Membranes were washed in TBST and incubated with appropriate secondary antibodies. The G:Box system (Syngene) was used to detect the signals from the membranes.

Immunofluorescence staining

Muscle sections were blocked with 2% FBS in 1xPBS for 30 min. The sections were incubated with primary antibodies against human-specific spectrin (1:50 mouse monoclonal IgG2b NCL-spec1, Novocastra, Leica Biosystems, Wetzlar Germany) human-specific lamin A/C (1:300 mouse monoclonal IgG1 Ab40567, Abcam, Cambridge, UK), or laminin (1:400 diluted, Z0097, Dako) for 1 hour and further incubated with appropriate secondary antibodies for 1 hour. When necessary, βgal detection was performed using a chicken antibody (Invitrogen AB9361; 1:1000; 1 hour). Pax7 staining was performed using a mouse monoclonal antibody (Developmental Studies Hybridoma Bank, Iowa City, IA; 1:20) after a 10 min fixation with 4% paraformaldehyde. Fiber type composition was obtained using an anti-MYHC-I antibody (A4.840, 1:50; DSHB) and an anti-MYHC-II (A4.74, 1:50; DSHB). Macrophages and neutrophils were stained with F4/80 antibody (MCA497BB, 1:50, Biorad) and Ly6g antibody (Ab25377, 1:100, Abcam) respectively, after a 10 min fixation with 4% paraformaldehyde. Finally, the sections were incubated 10 min with Hoechst (0.5µg/ml, Hoechst No. 33258; Sigma-Aldrich) and mounted with a mounting medium (Cytomation fluorescent mounting Medium, S3023, Dako, Agilent).

Vector genome quantification

Transduction efficacy was evaluated by quantification of viral genomes in injected muscles. Genomic DNA was extracted from mouse muscles using Puregene Blood kit (Qiagen, Courtaboeuf, France) according to the manufacturer's protocol. Copy numbers of AAV

genome and genomic DNA were measured on 100ng of genomic DNA by absolute quantitative real-time PCR on a StepOnePlus^{TM} (Applied Biosystems) using Taqman probe and the Taqman^{R}Universal Master Mix (Applied Biosystems)

To specifically amplify the viral genome sequence, we used the same primers as the one for AAV titration (above). A control pAAV plasmid was 10-fold serially diluted (from 10^7 to 10^1 copies) and used as a control to establish the standard curve for absolute quantification. All genomic DNA samples were analyzed in duplicates.

Statistical analysis

All data are mean values ± standard error of the mean. Statistical analyses were performed using the Student *t*-test or the one-way ANOVA with the Bonferroni post-hoc analysis as indicated. GraphPad Prism (version 4.0b; GraphPad Software, San Diego California, USA) was used for the analyses. A difference was considered to be significant at *$P < 0.05$, **$P < 0.01$ or ***$P < 0.001$.

Results

Transduction efficiency in mice

We first investigated the transduction efficiency of single stranded rAAV serotypes by local injection in skeletal muscle of control C57BL/6 mice. We used a CMV-nls-LacZ reporter cassette to precisely localize transduced nuclei. 10 different serotypes of rAAV-CMV-nls-LacZ (1, 2, 3, 4, 5, 6, 7, 8, 9 and 10) each at 3.5×10^{10} vector genomes (vg) were injected in the *tibialis anterior* (TA) of control C57BL/6 mice. Four weeks after injection, muscles were harvested and frozen for histological and biochemical analysis **(figure 1A)**. For each transduced TA, reporter nls-LacZ expression was quantified on the largest cross section area of the muscle by manual counting of all lacZ-positive nuclei **(figure 1B and supp figure 1A-B)** and by Western Blot **(supp figure 2A)**. The number of vector genomes was quantified by quantitative PCR (qPCR) **(supp figure 2B).** Four weeks post-injection, serotype 9 showed the most robust transduction **(figure 1C)**. All serotypes, except rAAV6, showed a limited inflammatory response. It should be noted that all of the rAAV6-injected TA's presented an intense inflammatory response with large areas of regenerating myofibers **(supp figure 2C),** thus maybe impairing the quantification of transduction efficiency. This was observed in independent experiments.

Transduction efficiency in human muscle using xenograft model

In order to evaluate intramuscular AAV transduction in a human context, we used a human muscle xenograft model: we transplanted fresh human skeletal muscle into the empty tibial compartment of Rag2−/− Il2rb−/− immunodeficient mice. Four months post-transplant, the engrafted human muscle regenerated as previously described [29]. Xenografts were composed entirely of human myofibers (expressing spectrin) **(figure 2B)** with comparable fiber type composition compared to the original donor biopsy **(Supp figure 3A-B)**. rAAV 8 and 9 vectors expressing CMV-nls-LacZ were injected into these xenografts, and mice were analyzed 4 weeks later **(figure 2A)**. These AAVs were selected as they showed a good efficiency in mouse and are currently being tested in several clinical trials for muscular dystrophy in patients. The position of the human xenografts was confirmed by immunofluorescence staining using anti-human spectrin and anti-human lamin A/C antibodies to stain specifically human muscle fiber membranes and human nuclei, respectively **(figure 2B and Supp figure 3C).** In human muscle xenografts, rAAV8 and rAAV9 gave comparable transduction efficiency **(figure 2C-D)** and transduced both slow and fast fibers **(figure 2E)**.

When compared to mouse, we observed a similar level of transduction for both rAAV serotypes **(figure 2F)** even though there is significant muscle fibrosis in the human xenograft **(figure 2G)**. Interestingly, we never observed LacZ expression in the human interstitial cells surrounding the muscle fibers **(figure 2H)**.

Discussion

Achieving efficient transduction of rAAV in diseased skeletal muscle, notably in the presence of fibrosis, is a major challenge for the treatment of muscular dystrophies. For many dystrophies a systemic administration of the vector is required, however for some more localized diseases a local intramuscular rAAV delivery might be sufficient. Whereas the comparison of serotypes has been largely described via systemic delivery, to our knowledge very few studies have compared their efficiency after a local intramuscular injection. In addition, while it is known that the potency of rAAV gene delivery can be impacted by several host factors, such as the molecular interactions between the capsid and target cell surface receptors [30] or the interaction with serum proteins in the circulation [31], the impact of fibrosis by extracellular matrix deposition around muscle fibers on rAAV transduction efficiency and the transduction of interstitial fibrosis cells has not been evaluated.

In this study we therefore tested the efficiency of rAAV1 to 10 after direct intramuscular injection into the TA of mice and human xenografted muscle.

When comparing the rAAVs in mouse we found that rAAV9 was the most efficient vector. Serotypes 1, 7 and 8 were also efficient although less so following intramuscular injection. rAAV1 gave high number of vector copy genome not correlated with high level of expression suggesting impaired disassembly in the nucleus as previously shown in Hela cells [32]. In the human xenograft model, rAAV8 and rAAV9 were found to be equally efficient at transducing both slow and fast human muscle fibers. It should be noted that rAAV9 and rAAV8 are already used in several ongoing clinical trials using systemic delivery in different myopathies: a Phase I/II trial with Solid Biosciences (NCT03368742) and one with Pfizer (NCT03362502) for DMD as well as a trial for Spinal muscular atrophy type 1 (NCT02122952) and a trial for X-linked Myotubular Myopathy (NCT03199469).

In our study, rAAV6-injected muscles systematically presented an acute inflammatory response with the degeneration and regeneration of the majority of the muscle fibers. Such a phenotype has been described previously for other transgenes [33–35] even though rAAV6 has also been used to transduce skeletal muscle [36–38]. As suggested by Winbanks et al, discrepancies in rAAV6 transduction and related inflammatory response could be due either to the nature of the transgene or to the dose used [38]. Regarding the nature of the transgene, the absence of an inflammatory response with all of the other rAAV serotypes used in our study suggests that the lacZ reporter gene is not itself deleterious. Regarding the dose, the question remains as to whether a lower dose of AAV6 would have allowed a better level of expression

without any related inflammatory response. We can only conclude here that at this same dose rAAV6 induces an inflammatory response whereas other serotypes do not, and this is not related to the quality of the rAAV6 production (data not shown).

AAV use glycan receptors and co-receptors, which play a role in cell attachment, and these interactions have been well characterized for a number of serotypes [30]: α2-3 and α2-6 N-linked sialic acid for AAV1 ; heparan sulfate proteoglycan for AAV 2 and 3 ; α2-3 O-linked and α2-3 N-linked sialic acids for AAV 4 and 5 ; heparan sulfate and α2-3 and α2-6 N-linked sialic acid for AAV6 ; and N-linked galactose for AAV9. A "new" cellular AAV receptor (AAVR, also named KIAA0319L) has also recently been described as essential for AAV cell entry following attachment [39,40]. In our study, none of the vectors were able to induce the expression of LacZ in interstitial cells (fibroblasts and inflammatory cells) (**figure 2H**) or satellite cells (**supp figure 4**), as previously described for rAAV6 [36] and rAAV9 [41,42]. We cannot exclude that these cells are transduced but unable to express the transgene, maybe due to an uncoating issue. Otherwise, this could be due to differences in cell surface receptors or mitotic status of myogenic and non-myogenic cells respectively. Further studies should include the analysis of the expression of these receptors on non myogenic/fibrotic cells compared to myogenic cells. Although we do not see any satellite cells targeted in our study, other have shown an efficient AAV transduction after systemic delivery with a CMV promoter [43]. An important feature of our study is the observation that the fibrosis present in the muscle xenograft does not impair rAAV8 and rAAV9 transduction of muscle fibers which is promising for future gene therapy strategies. Interestingly, rAAV transduction does not allow expression in interstitial muscle cells and further studies should look at other vectors which could target these non myogenic cells with a potential anti-fibrotic gene therapy purpose. Elucidating tropism and transduction efficiency is critical to implement targeted and specific applications in a dynamic environment such as pathological muscle.

It is always a challenge to translate results obtained in mice into larger species. For example different profiles have been observed between transduction efficiency in mice and dogs [44]. We used for the first time a muscle xenograft model to evaluate AAV transduction efficiency in a human context. We did not observe any difference between rAAV8 and rAAV9 confirming their efficient transduction profile in human muscle. Interestingly, while different transduction efficiency have been observed on different fiber types in mice [33,45] we observed transduction of both slow and fast fiber type in the xenograft model. While bearing in mind that the human xenograft corresponds to a regenerated human muscle, we believe that this xenograft model is an ideal tool for pre-clinical studies to translate results found in mice into an *in vivo* human

context and to further validate therapeutic strategies. The presence of a high degree of fibrosis in these xenografts could be a very useful model to evaluate therapeutic gene-based strategies in a fibrotic environment, similar to that observed in most muscular dystrophies.

Author disclosure statement

No competing financial interests.

References

1.   Colella P, Ronzitti G, Mingozzi F. Emerging Issues in AAV-Mediated In Vivo Gene Therapy. Molecular Therapy - Methods & Clinical Development 2018;8:87–104.
2.   Wang D, Tai PWL, Gao G. Adeno-associated virus vector as a platform for gene therapy delivery. Nature Reviews Drug Discovery . Epub ahead of print February 1, 2019. DOI: 10.1038/s41573-019-0012-9.
3.   Xiao W, Chirmule N, Berta SC, et al. Gene therapy vectors based on adeno-associated virus type 1. J Virol 1999;73:3994–4003.
4.   Srivastava A, Lusby EW, Berns KI. Nucleotide sequence and organization of the adeno-associated virus 2 genome. Journal of Virology 1983;45:555–564.
5.   Muramatsu S-I, Mizukami H, Young NS, et al. Nucleotide Sequencing and Generation of an Infectious Clone of Adeno-Associated Virus 3. Virology 1996;221:208–217.
6.   Chiorini JA, Yang L, Liu Y, et al. Cloning of adeno-associated virus type 4 (AAV4) and generation of recombinant AAV4 particles. Journal of Virology 1997;71:6823–6833.
7.   Chiorini JA, Kim F, Yang L, et al. Cloning and characterization of adeno-associated virus type 5. J Virol 1999;73:1309–1319.
8.   Rutledge EA, Halbert CL, Russell DW. Infectious clones and vectors derived from adeno-associated virus (AAV) serotypes other than AAV type 2. J Virol 1998;72:309–

319.

9.   Gao G-P, Alvira MR, Wang L, et al. Novel adeno-associated viruses from rhesus monkeys as vectors for human gene therapy. Proc Natl Acad Sci USA 2002;99:11854–11859.

10.   Gao G, Vandenberghe LH, Alvira MR, et al. Clades of Adeno-associated viruses are widely disseminated in human tissues. J Virol 2004;78:6381–6388.

11.   Mori S, Wang L, Takeuchi T, et al. Two novel adeno-associated viruses from cynomolgus monkey: pseudotyping characterization of capsid protein. Virology 2004;330:375–383.

12.   Grimm D, Zhou S, Nakai H, et al. Preclinical in vivo evaluation of pseudotyped adeno-associated virus vectors for liver gene therapy. Blood 2003;102:2412–2419.

13.   Paulk NK, Pekrun K, Zhu E, et al. Bioengineered AAV Capsids with Combined High Human Liver Transduction In Vivo and Unique Humoral Seroreactivity. Molecular Therapy 2018;26:289–303.

14.   Halbert CL, Allen JM, Miller AD. Adeno-associated virus type 6 (AAV6) vectors mediate efficient transduction of airway epithelial cells in mouse lungs compared to that of AAV2 vectors. J Virol 2001;75:6615–6624.

15.   Auricchio A, Smith AJ, Ali RR. The Future Looks Brighter After 25 Years of Retinal Gene Therapy. Hum Gene Ther 2017;28:982–987.

16.   Harper SQ, Hauser MA, DelloRusso C, et al. Modular flexibility of dystrophin: implications for gene therapy of Duchenne muscular dystrophy. Nat Med 2002;8:253–61.

17.   Greelish JP, Su LT, Lankford EB, et al. Stable restoration of the sarcoglycan complex in dystrophic muscle perfused with histamine and a recombinant adeno-associated viral vector. Nat Med 1999;5:439–443.

18.   Ellis BL, Hirsch ML, Barker JC, et al. A survey of ex vivo/in vitro transduction efficiency of mammalian primary cells and cell lines with Nine natural adeno-associated virus (AAV1-9) and one engineered adeno-associated virus serotype. Virol J 2013;10:74.

19.   Gregorevic P, Blankinship MJ, Allen JM, et al. Systemic delivery of genes to striated muscles using adeno-associated viral vectors. Nat Med 2004;10:828–834.

20.   Wang Z, Zhu T, Qiao C, et al. Adeno-associated virus serotype 8 efficiently delivers genes to muscle and heart. Nat Biotechnol 2005;23:321–328.

21.   Zincarelli C, Soltys S, Rengo G, et al. Analysis of AAV Serotypes 1–9 Mediated Gene Expression and Tropism in Mice After Systemic Injection. Mol Ther 2008;16:1073–1080.

22.   Brais B, Bouchard JP, Xie YG, et al. Short GCG expansions in the PABP2 gene cause oculopharyngeal muscular dystrophy. Nat Genet 1998;18:164–7.

23.   Gidaro T, Negroni E, Perié S, et al. Atrophy, Fibrosis, and Increased PAX7-Positive Cells in Pharyngeal Muscles of Oculopharyngeal Muscular Dystrophy Patients. J Neuropathol Exp Neurol 2013;72:234–243.

24.   Malerba A, Klein P, Bachtarzi H, et al. PABPN1 gene therapy for oculopharyngeal muscular dystrophy. Nat Commun 2017;8:14848.

25.   Duan D. Systemic AAV Micro-dystrophin Gene Therapy for Duchenne Muscular Dystrophy. Mol Ther 2018;26:2337–2356.

26.   Serrano AL, Muñoz-Cánoves P. Regulation and dysregulation of fibrosis in skeletal muscle. Exp Cell Res 2010;316:3050–3058.

27.   Wynn TA. Cellular and molecular mechanisms of fibrosis. J Pathol 2008;214:199–210.

28.   Grieger JC, Choi VW, Samulski RJ. Production and characterization of adeno-associated viral vectors. Nature Protocols 2006;1:1412–1428.

29.   Zhang Y, King OD, Rahimov F, et al. Human skeletal muscle xenograft as a new preclinical model for muscle disorders. Hum Mol Genet 2014;23:3180–3188.

30.   Huang L-Y, Halder S, Agbandje-McKenna M. Parvovirus glycan interactions. Current Opinion in Virology 2014;7:108–118.

31.   Denard J, Rouillon J, Leger T, et al. AAV-8 and AAV-9 Vectors Cooperate with Serum Proteins Differently Than AAV-1 and AAV-6. Molecular Therapy - Methods & Clinical Development 2018;10:291–302.

32.   Keiser NW, Yan Z, Zhang Y, et al. Unique Characteristics of AAV1, 2, and 5 Viral Entry, Intracellular Trafficking, and Nuclear Import Define Transduction Efficiency in HeLa Cells. Human Gene Therapy 2011;22:1433–1444.

33.   Riaz M, Raz Y, Moloney EB, et al. Differential myofiber-type transduction preference of adeno-associated virus serotypes 6 and 9. Skeletal Muscle;5 . Epub ahead of print December 2015. DOI: 10.1186/s13395-015-0064-4.

34.   Wang Z, Tapscott SJ, Chamberlain JS, et al. Immunity and AAV-Mediated Gene Therapy for Muscular Dystrophies in Large Animal Models and Human Trials. Frontiers in Microbiology;2 . Epub ahead of print 2011. DOI: 10.3389/fmicb.2011.00201.

35.   Arnett ALH, Garikipati D, Wang Z, et al. Immune Responses to rAAV6: The Influence of Canine Parvovirus Vaccination and Neonatal Administration of Viral Vector. Frontiers in Microbiology;2 . Epub ahead of print 2011. DOI: 10.3389/fmicb.2011.00220.

36.   Arnett AL, Konieczny P, Ramos JN, et al. Adeno-associated viral vectors do not efficiently target muscle satellite cells. Molecular Therapy - Methods & Clinical Development 2014;1:14038.

37.   Qiao C, Zhang W, Yuan Z, et al. Adeno-Associated Virus Serotype 6 Capsid Tyrosine-to-Phenylalanine Mutations Improve Gene Transfer to Skeletal Muscle. Human Gene Therapy 2010;21:1343–1348.

38.   Winbanks CE, Beyer C, Qian H, et al. Transduction of Skeletal Muscles with Common Reporter Genes Can Promote Muscle Fiber Degeneration and Inflammation. PLoS ONE 2012;7:e51627.

39.   Pillay S, Zou W, Cheng F, et al. Adeno-associated Virus (AAV) Serotypes Have Distinctive Interactions with Domains of the Cellular AAV Receptor. J Virol;91 . Epub ahead of print September 15, 2017. DOI: 10.1128/JVI.00391-17.

40.   Pillay S, Meyer NL, Puschnik AS, et al. An essential receptor for adeno-associated virus infection. Nature 2016;530:108–112.

41.   Stitelman DH, Brazelton T, Bora A, et al. Developmental stage determines efficiency of gene transfer to muscle satellite cells by in utero delivery of adeno-associated virus vector serotype 2/9. Molecular Therapy - Methods & Clinical Development 2014;1:14040.

42.   Nance ME, Shi R, Hakim CH, et al. AAV9 edits muscle stem cells in normal and dystrophic adult mice. Molecular Therapy;0 . Epub ahead of print July 3, 2019. DOI: 10.1016/j.ymthe.2019.06.012.

43.   Goldstein JM, Tabebordbar M, Zhu K, et al. In Situ Modification of Tissue Stem and Progenitor Cell Genomes. Cell Reports 2019;27:1254-1264.e7.

44.   Pan X, Yue Y, Zhang K, et al. AAV-8 is more efficient than AAV-9 in transducing neonatal dog heart. Hum Gene Ther Methods 2015;26:54–61.

45.   Bostick B, Ghosh A, Yue Y, et al. Systemic AAV-9 transduction in mice is influenced by animal age but not by the route of administration. Gene Therapy 2007;14:1605–1609.

Figure legends

Fig. 1. Intramuscular AAV transduction efficiency in control C57BL/6 mice. rAAV serotypes 1 to 10 were injected into the TA (3.5×10^{10} vg/TA) . Mice were sacrificed 4 weeks post-injection and TA were analyzed (N=4 to 10 TA) **A.** Cryostat sections of TA muscles of C57BL/6 mice injected with rAAV1 to 10 carrying a nls-LacZ gene reporter and stained for β-galactosidase activity and laminin. (scale bar: 250μm) **B.** Quantification of cross sectional β-galactosidase positive nuclei by mm^2 (N=4 to 10 TA) **C.** Transduction efficiency is expressed as the β-gal positive nuclei/mm^2 relative to the AAV genome copy (gc) number quantified by absolute Taqman qPCR. (*$P<0.05$, **$P<0.01$, ***$P<0.001$, ****$P<0.0001$ ANOVA Tukey test)

Fig. 2. Intramuscular AAV transduction efficiency in human xenograft. A. Experimental scheme depicting xenograft time course. Strips of human biopsies were xenografted into the empty tibial compartment of immunodeficient Rag2−/− Il2rb−/− mice. 4 months later, rAAV serotypes 8 and 9 (3×10^{10} vg/TA) were injected into the graft. Mice were sacrificed 4 weeks post-injection and muscles were analyzed **B**. Immunofluorescent staining of human spectrin (green), human lamin a/c (red) and laminin (blue) on a cryosection of human xenograft. **C.** Cryosection of xenograft injected with AAV8, stained for β-galactosidase and counterstained with Hematoxylin Eosin. (scale bar=100μm) **D.** Cryosection of xenograft injected with AAV9 and stained for β-galactosidase and colored with Hematoxylin Eosin. (scale bar =100μm) **E.** Fiber type (MyHCI-red and MyHCII-green) and β-galactosidase (blue) immunostaining on rAAV8- and rAAV9-injected xenograft. **F.** Quantification of cross sectional xenograft β-galactosidase positive nuclei related to fiber number on cross sectional human xenograft and compared to a C57BL/6 mouse injected with AAV8 and AAV9 (N=3). Anova Tukey Test. NS non significant **G.** Sirius red coloration of mouse muscle vs xenograft. Fibrosis was quantified with ImageJ software. ****$P<0,0001$, T test **H.** Cryosection of xenograft injected with AAV9, stained for β-galactosidase (blue) and stained with Hematoxylin Eosin. No β-gal+ interstitial cells are observed
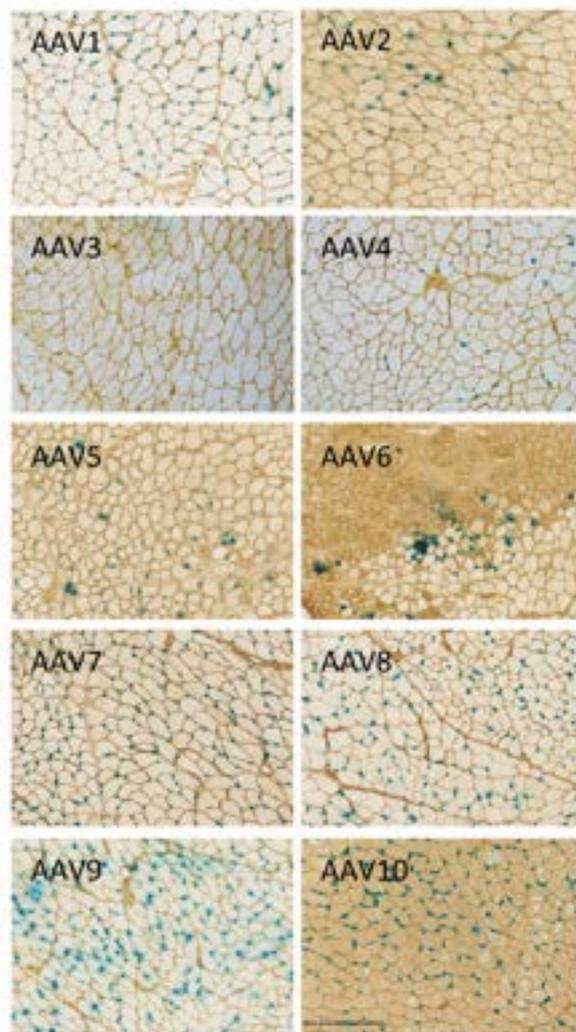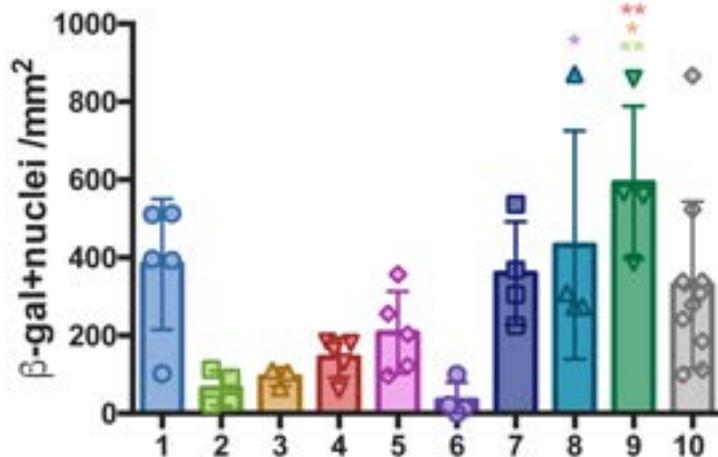
Supplementary Fig. 1. Intramuscular AAV transduction efficiency evaluation in control C57BL/6 mice. A. Schematic representation of the protocol performed to quantify β-galactosidase expression on injected TA muscle. Each section (5μm) on the same slide is separated from the previous and following one by 500μm. Quantification is performed on the

largest cross-sectional area (black circle). **B.** Representative whole TA muscle section with β-galactosidase activity (blue) and laminin (brown) staining for serotypes rAAV1 to rAAV10.

Supplementary Fig. 2. Evaluation of AAV transduction efficiency in control C57BL/6 mice. A. Western-blot analysis of β-galactosidase expression normalized to Tubulin. A representative Western-blot is presented on the left and densitometry quantification of β-galactosidase expression from 3 samples per condition. 'Non inj.' corresponds to a non injected leg as a control. **B.** AAV genome copy number per μg of DNA for each serotype (n=4-10) quantified by absolute Taqman qPCR. **C.** Hematoxylin Eosin coloration and immunofluorescent staining of dapi (blue), macrophages (green), neutrophils (red) and laminin (grey) in AAV injected muscles showing the intense inflammatory response in the AAV6 injected muscle compared to another AAV where no sign of inflammation was visible (here AAV8).

Supplementary Fig. 3. Human xenograft model. A. Comparison of human muscle before (original biopsy) and after (xenograft) grafting regarding fiber type**.** MyHCI (red), MyHCII (green) and laminin (blue). Scale bar = 50 μm**.** Quantification of MYHCI percentage on 4 biopsies before and after grating shows no difference. **B.** Cumulative distribution of fiber diameter comparing original biopsy and xenograft (4 month after grafting). **C.** Sirius red staining, fiber typing, hLaminAC/hSpectrin/dapi staining and H&E/ β-gal staining on the same muscle xenograft. The delineated area is the same as the one presented in figure 3D (H&E/ β-gal).

Supplementary Fig. 4. Transduction in muscle satellite cells. Immunofluorescent staining of DAPI (blue), laminin (grey), PAX7 (red) and β-gal (green) after injection of AAV9 in C57BL/6 mouse TA. No cells PAX7+/β-gal+ were observed following injection of all serotypes, neither in C57BL/6 nor SCID/beige/sgca-null mice (arrowhead points to PAX7+ satellite cells). Scale bar =100 μm

A

B hLaminin hSpectrin hLaminAC

C human AAV8

D human AAV9

E AAV8 AAV9 βgal MyHCI MyHCII

F β-gal+nuclei/ fiber number

G mouse graft % fibrosis *** mouse xenograft

H